

***A “Roller-Wheel” Pt-Containing Small Molecule
that Outperforms Its Polymer Analogs in Organic
Solar Cells***

**Wenhan He¹, Maksim Y. Livshits¹, Diane A. Dickie¹, Jianzhong
Yang¹, Rachel Quinnett², Jeffrey J. Rack¹, Qin Wu³, and Yang
Qin¹**

¹University of New Mexico, Albuquerque, NM 87131, USA

²Kansas State University, Manhattan, KS 66506, USA

³Brookhaven National Laboratory, Upton, NY 11973 USA

Submitted to Chemical Sciences

May 2016

Center for Functional Nanomaterials

Brookhaven National Laboratory

**U.S. Department of Energy
Office of Science, Basic Energy Sciences**

Notice: This manuscript has been co-authored by employees of Brookhaven Science Associates, LLC under Contract No. DE-SC0012704 with the U.S. Department of Energy. The publisher by accepting the manuscript for publication acknowledges that the United States Government retains a non-exclusive, paid-up, irrevocable, world-wide license to publish or reproduce the published form of this manuscript, or allow others to do so, for United States Government purposes.

DISCLAIMER

This report was prepared as an account of work sponsored by an agency of the United States Government. Neither the United States Government nor any agency thereof, nor any of their employees, nor any of their contractors, subcontractors, or their employees, makes any warranty, express or implied, or assumes any legal liability or responsibility for the accuracy, completeness, or any third party's use or the results of such use of any information, apparatus, product, or process disclosed, or represents that its use would not infringe privately owned rights. Reference herein to any specific commercial product, process, or service by trade name, trademark, manufacturer, or otherwise, does not necessarily constitute or imply its endorsement, recommendation, or favoring by the United States Government or any agency thereof or its contractors or subcontractors. The views and opinions of authors expressed herein do not necessarily state or reflect those of the United States Government or any agency thereof.

A "Roller-Wheel" Pt-Containing Small Molecule that Outperforms Its Polymer Analogs in Organic Solar Cells

Wenhan He,^a Maksim Y. Livshits,^a Diane A. Dickie,^a Jianzhong Yang,^a Rachel Quinnett,^b Jeffrey J. Rack,^a Qin Wu^c and Yang Qin*^a

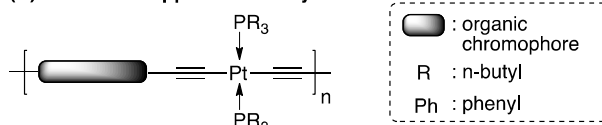
A novel Pt-bisacetylde small molecule (**Pt-SM**) featuring "roller-wheel" geometry was synthesized and characterized. When compared with conventional Pt-containing polymers and small molecules having "dumbbell" shaped structures, **Pt-SM** displays enhanced crystallinity and intermolecular π - π interactions, as well as favorable panchromatic absorption behaviors. Organic solar cells (OSCs) employing **Pt-SM** achieve power conversion efficiencies (*PCEs*) up to 5.9%, the highest reported so far for Pt-containing polymers and small molecules.

Introduction

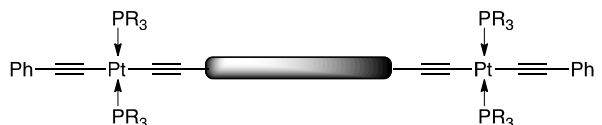
Organic solar cells (OSCs) have been widely perceived as low-cost alternative energy sources that possess unique properties including light-weight, flexibility and semi-transparency.¹ State-of-the-art OSCs, with power conversion efficiencies (*PCEs*) now beyond 10%,²⁻⁸ contain blends of an organic light-absorbing electron donor and a fullerene derivative as the electron acceptor, forming bulk heterojunction (BHJ) morphologies that play a decisive role on device performance.⁹⁻¹⁰ Steady improvements in OSC efficiencies have resulted mainly from rational design and synthesis of conjugated donor materials,¹¹⁻¹² interfacial engineering,¹³⁻¹⁴ novel device geometries,¹⁵⁻¹⁶ as well as morphology optimization via Edisonian approaches including thermal/solvent annealing and additives.¹⁷⁻¹⁸ Another intriguing but less explored strategy is to incorporate heavy metals into the organic materials, leading to facile formation of triplet excitons. The extended lifetimes and thus longer diffusion lengths of triplet excitons have been suggested to improve the charge separation efficiency.¹⁹⁻²⁷ Among the various examples of metal-containing materials applied in OSCs, conjugated polymers (CPs) containing main-chain Pt-bisacetylde moieties, having the general structures shown in Scheme 1A, are the most studied.²⁸⁻³⁰ Besides a handful of examples showing moderate *PCEs* of ca. 2-4%,³¹⁻³⁵ most such Pt-containing CPs display relatively low performance, which

has been mainly ascribed to their intrinsic amorphous nature, resulting in low conductivity and unfavorable BHJ morphologies.³⁶⁻³⁹

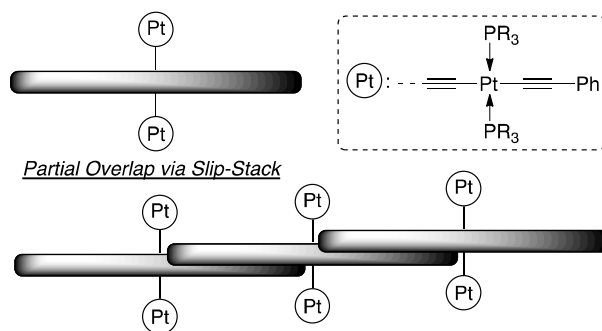
(A) Traditional Approach in Polymers



(B) Traditional Approach in Small Molecules: "Dumbbell" Shaped



(C) Our Approach in Small Molecules: "Roller-Wheel" Shaped



Scheme 1. Structures of Pt-Bisacetylde Materials.

Although less explored in OSC applications, conjugated small molecules (SMs) can be highly crystalline and thus have superior charge mobilities, as well as discrete and reproducible molecular structures.⁴⁰⁻⁴¹ These features have attracted increasing attention and OSC devices employing conjugated SMs have been constantly improved to rival their CP counterparts.^{4,42} On the other hand, conjugated SMs

^a Department of Chemistry & Chemical Biology, University of New Mexico, MSC03 2060, 1 UNM, Albuquerque, NM 87131, USA.

^b Department of Chemical Engineering, Kansas State University, 1005 Durland Hall, Manhattan, KS 66506, USA.

^c Center for Functional Nanomaterials, Brookhaven National Laboratory, PO Box 5000, Upton, NY 11973, USA.

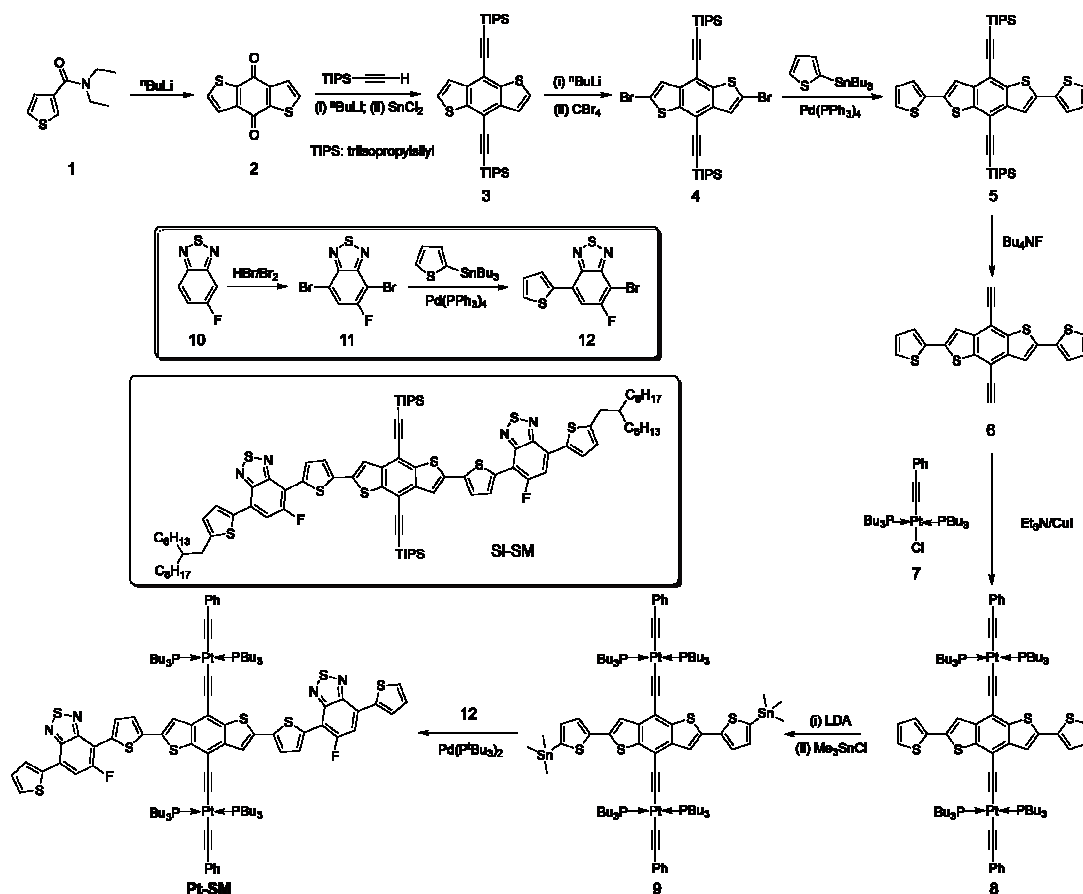
Electronic Supplementary Information (ESI) available: detailed synthetic procedures, DSC, XRD, absorption, CV and NMR spectra. See DOI: 10.1039/x0xx00000x

containing Pt-bisacetylides, having typical structures as shown in Scheme 1B, are mostly prepared as model compounds, resembling their polymeric analogs, for photophysical studies.⁴³⁻⁴⁴ These SMs, similar to their polymeric analogs, possess "dumbbell" shaped molecular structures having bulky Pt groups at both ends of linear organic chromophores, resulting in inefficient molecular packing and π - π interactions. We propose a new structural design, as shown in Scheme 1C, having Pt-bisacetylides as side-chains attached at the center of a rigid and linear conjugated chromophore. This "roller-wheel" shaped structure can allow partial overlap among adjacent chromophores in a slip-stacked fashion similar to that observed in symmetrically substituted acenes,⁴⁵⁻⁴⁶ potentially enhancing crystallinity and conductivity. Herein, we report the synthesis, characterization and OSC application of such a "roller-wheel" molecule, **Pt-SM** that generates *PCEs* up to ca. 5.9% in BHJ devices, the highest reported so far for Pt-containing SMs and polymers.

Results and Discussion

Synthetic procedures toward the target compound **Pt-SM** are outlined in Scheme 2 and the structure of **Si-SM**, the non-

metallic analog to **Pt-SM** by replacing the Pt-containing moieties with tris(isopropyl)silyl (TIPS) groups is also shown. Synthetic details are included in the Electronic Supplementary Information (ESI[†]). The alkyl side-chains on **Si-SM** are necessary for solution processability, since attempts to prepare **Si-SM** analogs having no side-chains at both terminal thiophene rings led to materials that are poorly soluble in common organic solvents and difficult to purify and analyze. On the other hand, the four bulky tri(*n*-butyl)phosphine ligands make **Pt-SM** readily soluble in common organic solvents such as CHCl_3 , chlorobenzene, toluene and THF, *etc.*, without the need for additional alkyl side-chains. **Pt-SM** is fully characterized by ^1H , ^{13}C , ^{19}F and ^{31}P NMR spectroscopy, as well as high resolution mass spectrometry (HR-MS). Although we have not been able to obtain high quality single crystals for precise structure determination, certain crystallinity of **Pt-SM** can be observed in differential scanning calorimetry (DSC) and thin film X-ray diffraction (XRD) measurements. As shown in the DSC trace in Figure S1A (see ESI[†]), a clear, reproducible melting transition peak at 114 °C is seen. Figure S1B (see ESI[†]) displays several sharp XRD signals from **Pt-SM** films drop-cast onto glass substrates. Although accurate assignments of these peaks are difficult, the signal at $2\theta = 23.3^\circ$ corresponds to a *d*-spacing of ca. 3.81 Å, which is characteristic of typical π - π



Scheme 2. Synthesis of Pt-SM and Structure of Si-SM.

stacking distances of aromatic molecules.⁴⁷ Such π - π stacking motifs are important for electronic coupling among adjacent chromophores and for efficient exciton/charge transport. Both the DSC and XRD measurements suggest that **Pt-SM** possesses certain crystallinity, which has rarely been observed in Pt-bisacetylide containing SMs and polymers.⁴⁸

For a better comparison, we also studied the physical properties of the structurally similar **Si-SM** and compound **8** (Scheme 2) in detail. Figure S2 (see ESI[†]) shows the DSC traces (2nd heating) of these two compounds. Both **Si-SM** and **8** possess higher melting points at 243 °C and 204 °C, respectively, than that of **Pt-SM**. We have also not been able to obtain single crystals of **Si-SM** and its XRD pattern is shown in Figure S3 (see ESI[†]). Only one scattering signal at $2\theta = 4.18^\circ$, corresponding to a d -spacing of 2.11 nm, can be observed, which indicates less crystalline order for **Si-SM** likely caused by the large branched alkyl side-chains. On the other hand, we did obtain single crystals of compound **8** and the crystal structures and molecular packing motifs are displayed in Figure S4 (see ESI[†]). Noticeably, although the conjugated chromophores are nearly planar and parallelly aligned, they are slip-stacked from each other along the short axis with tri-*n*-butylphosphine groups situated in between. Such packing geometry leads to an inter-chromophore distance of ca. 7.59 Å that is too large for efficient π - π interactions and charge transport (*vide infra*).

The electronic properties of **Pt-SM** were first studied by using density functional theory (DFT) and the results are summarized in Figure 1. All non-essential side chains are replaced with H atoms for computation efficiency and the ground state geometries are optimized using DFT, while the excited states are calculated with linear response time-dependent DFT (TD-DFT)⁴⁹⁻⁵⁰ at the optimized ground state geometries only. All calculations are performed with the Gaussian 09 package (Rev. B.01)⁵¹ using the hybrid B3LYP functional. The 6-31G* basis set is used for all atoms except for Pt, which has the LANL2DZ basis set for its 5s, 5p, 5d, and 6s valence electrons while the core electrons are replaced by the corresponding pseudopotential.⁵² A solvent reaction field simulated by the default polarizable continuum model (PCM) is also employed.⁵³ We then use the natural transition orbital (NTO) approach⁵⁴ to characterize the nature of the lowest singlet and triplet states. We first examined the bright singlet states in **Pt-SM** that are the S1 and S3 states having transition energies at 1.59 eV and 2.02 eV, respectively. From these NTOs that approximately represent the hole and electron in the transitions, both the S1 and S3 states have clear charge transfer characters mixed with metal-to-ligand-charge-transfer (MLCT) transitions, as expected from the electron rich benzenedithiophene (BDT) core and electron poor fluorinated benzothiadiazole (F-BTD) arms, as well as the hole density delocalized throughout the Pt-bisacetylide moieties. We then examine the triplet states in **Pt-SM**. It should be noted that the NTOs for these triplet states are only the dominant representation (given in percentages), unlike the singlet transition in Figure 1 where the NTOs represent 100% of the transitions. There are two triplet states having energies lower

than S1, which are the T1 (1.14 eV) and T2 (1.25 eV) states. The T1 state is delocalized along the organic chromophore while the T2 state has obvious charge transfer character with spin density more localized on the F-BTD moieties. The third triplet state, T3, lies at 1.60 eV, *i.e.*, less than 10 meV higher than that of S1. It is therefore plausible that an efficient intersystem crossing occurs at S1 and T3.⁵⁵ T3 then fast decays into either T1 or T2, or both states, which then respectively decay to the ground state either single exponentially (from T1 or T2) or biexponentially (from both T1 and T2).

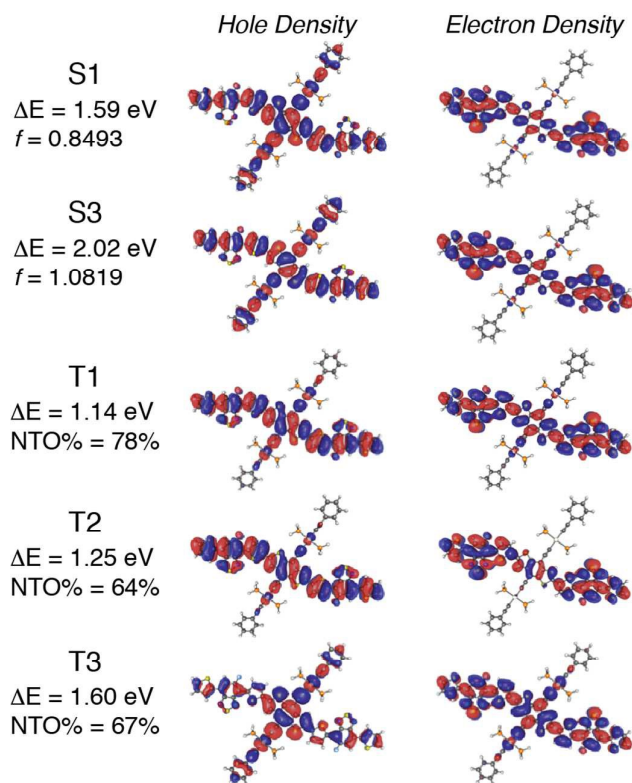


Figure 1. Low-lying bright singlet states and triplet states of **Pt-SM** calculated by density functional theory (DFT). ΔE : transition energy; f : oscillator strength; NTO: natural transition orbital.

The UV-vis absorption and emission spectra of **Pt-SM** in both dilute solutions and as thin films are shown in Figure 2. Multiple absorption peaks at ca. 323, 364, 442, 487 and 560 nm are observed in dilute chlorobenzene solutions of **Pt-SM**. From the absorption onset at ca. 642 nm, the solution bandgap of **Pt-SM** is estimated to be ca. 1.93 eV. Upon casting into thin films, the absorption profile of **Pt-SM** experiences significant red-shifts, leading to an onset of ca. 692 nm and an estimated solid-state bandgap of ca. 1.79 eV. Intriguingly, the films of **Pt-SM** display panchromatic behavior with strong absorption covering a large spectroscopic range from 300 nm to 700 nm, having multiple peaks at ca. 362, 432, 458, 523, 583 and 642 nm. It is not clear at this stage whether these peaks may be vibronic in nature or if they originate from different electronic transitions as suggested by DFT calculations. This question merits more detailed studies in the future. In order to qualitatively probe the origins of these electronic transitions, we also performed absorption and emission

measurements of **Si-SM** and compound **8** under identical conditions. As shown in Figure S5 (see ESI[†]), **Si-SM** displays a dominant structureless peak at 517 nm in solutions, becoming structured and red-shifted to 606 nm in thin films, which is absent for compound **8**. This low energy transition has been assigned to intramolecular charge-transfer (ICT) from the electron rich BDT centers to the electron poor F-BTD groups, as shown in recent examples with similar structures.⁵⁶⁻⁵⁹ We thus assign the low energy absorption peaks observed for **Pt-SM** to similar ICT transitions, which is consistent with our DFT calculations. Noticeably, these ICT transitions of **Pt-SM** are at lower energies respectively than those of **Si-SM**, suggesting electronic contribution to the ICT transitions from the Pt moieties through MLCT as suggested by the DFT calculations.

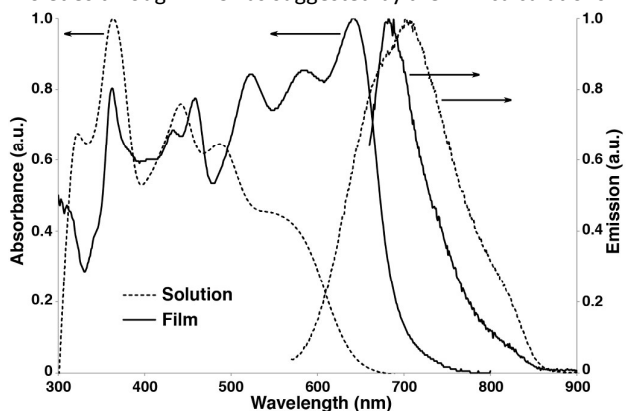


Figure 2. UV-vis absorption and emission spectra of **Pt-SM** in chlorobenzene solutions (10^{-2} M, dashed lines) and as thin films (solid lines).

Furthermore, spectral red-shift from solution to thin film is only observed for **Pt-SM** and **Si-SM**, but not for **8**, indicating better molecular packing, and thus enhanced inter-molecular electronic interactions, for the first two compounds but otherwise for the latter. This observation is consistent with the XRD and crystal structure studies for **Pt-SM** and **8**, respectively. Compared with **8**, **Pt-SM** has identical bulky Pt-BDT center unit but more extended arms. The absorption profiles are thus consistent with our hypothesis that the "roller-wheel" structures can allow partial overlap and π - π interactions among adjacent molecules if the "roller-wheel handles" are long enough.

Pt-SM shows very weak emissions peaked at ca. 700 nm in solutions (excited at 560 nm) and at ca. 680 nm as thin films (excited at 642 nm), respectively. The slight blue shift of the emission in thin films from that of the solutions is presumably due to H-type aggregation of the chromophores,⁶⁰⁻⁶¹ which is consistent with our conjecture on the solid-state structure of **Pt-SM**. The lifetime of these emissions was measured to be ca. 330 ps and did not change with or without the presence of oxygen. Also based on the relatively small Stokes shift, we assign the emissions of **Pt-SM** to fluorescence. The solution fluorescence quantum yield (QY) of **Pt-SM** is estimated to be ca. 0.77%, while the solution QY of **Si-SM** is calculated to be ca. 6.6%. This significant reduction in QY for **Pt-SM** is possibly caused by the attachment of Pt atoms, leading to increased intersystem crossing (ISC) rates. No phosphorescence could be

observed for **Pt-SM** solutions or thin films even when cooled down to 10 K. Such lack of phosphorescence has been observed in previously reported Pt-containing low bandgap CPs and small molecules,³¹⁻³⁵ which is commonly ascribed to the energy gap law.⁶² Noticeably, compound **8** does display a phosphorescence peak at ca. 705 nm in deaerated solutions that disappears when open to air (Figure S5, see ESI[†]).

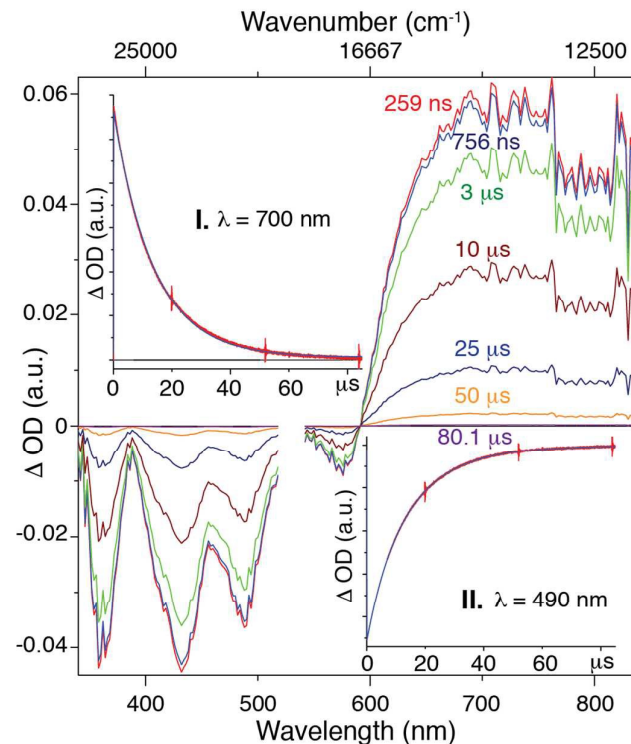


Figure 3. Transient absorption spectra of **Pt-SM** collected in chlorobenzene, excited at 532 nm with a nanosecond pulse from a SHG Continuum Surelight Nd:YAG at 1 Hz. The data near the excitation wavelength have been omitted for clarity. The transient spectrum was collected at 250 ns followed sequentially by transient spectra at 750 ns, 3 μ s, 10 μ s, 25 μ s, 50 μ s and 80 μ s. Insert: single wavelength kinetic traces (red) and fits (blue) at 700 nm (I) and 490 nm (II).

Although we are not able to directly observe phosphorescence from **Pt-SM**, the presence of ISC events and triplet states have been demonstrated by using transient absorption spectroscopy as shown in Figure 3. The 750 ns transient absorption spectrum of **Pt-SM** features four negative or bleach peaks from 340 nm to 600 nm, and a broad excited state absorption from 600 nm to 850 nm. The four bleach peaks are ascribed to loss of the ground state, as they are consistent with the absorption spectrum of **Pt-SM** (Figure 2). We ascribe the excited state absorption feature to two different triplet transitions, as reported in similar systems,^{24-25,30,37} and supported by our DFT calculations. Single wavelength kinetics collected at 700 nm and 490 nm, as respectively shown in inserts I and II of Figure 3, retrieved time constants of 7.5 ± 0.4 μ s and 16.3 ± 0.4 μ s. These are in good agreement with lifetimes of 7.6 ± 0.35 μ s and 16.4 ± 0.27 μ s, obtained from global fitting analysis. We ascribe the 7.5 μ s time constant observed in the transient kinetics to a triplet charge separated state from the BDT core to the F-BTD arms, *i.e.*, the T2 state from DFT calculations. The 16.5 μ s transition is thus ascribed

to the T1 triplet state that is more delocalized. We make these assignments based upon independent transient absorption spectroscopic measurements of the compound **8** and **Si-SM**. The lifetime of the 700 nm transient absorption of **Si-SM** is fit to a single exponential of 1.6 μ s and that of **8** (700 nm) is fit to a lifetime of 14.7 μ s, respectively. This observation is consistent with DFT calculations, which find two triplet states of different origins in close energy (ca. 0.1 eV) to each other.

The HOMO and LUMO levels of **Pt-SM** were estimated using cyclic voltammetry (CV) as shown in Figure S6 (see ESI[†]). One pseudo-reversible reduction and two oxidation peaks are observed, from the onsets of which, the HOMO and LUMO levels are estimated to be ca. -5.0 eV and -3.2 eV, respectively, leading to an electrochemical bandgap of ca. 1.8 eV that agrees well with the optical measurements.

One key parameter of organic materials for electronic devices is the charge mobility. We have measured hole mobilities of **Pt-SM**, **Si-SM** and compound **8** using space charge limited current (SCLC) method.⁶³ Hole selective device geometries (ITO/MoO₃/organic/MoO₃/Al) are employed and the current density-voltage (I-V) curves are shown in Figure S7 (see ESI[†]). From the linear region of each I-V curve, the hole mobilities of **Pt-SM**, **Si-SM** and **8** are estimated to be 1.5×10^{-5} cm²/V•s, 1.6×10^{-5} cm²/V•s and 1.6×10^{-6} cm²/V•s, respectively. Although single crystalline in the solid state, **8** displays one order of magnitude lower hole mobility. This is expected from the crystal structure in which there is no efficient π - π overlap among adjacent chromophores for charge transport and agrees well with the nearly identical solution and film absorption profiles. On the other hand, **Pt-SM** and **Si-SM** show similarly enhanced charge mobilities, indicating better solid state packing structures and more efficient π - π stacking among adjacent conjugated chromophores.

OSC devices were fabricated using **Pt-SM**, **Si-SM** and compound **8** in device geometries: ITO glass/MoO₃ (10 nm)/organic blend layer/Al (100 nm). The devices were first optimized using blends of phenyl-C₆₁-butyric acid methyl ester (PC₆₁BM) by varying the donor/acceptor weight ratios, solvent choices, solution concentrations, spin-coating conditions and thermal/solvent annealing conditions. Table S1 summarizes representative device parameters of **Pt-SM** from various optimization conditions and Table S2 gives the optimized device performances of **Si-SM** and **8** (see ESI[†]). The best devices were found to use a **Pt-SM**/PC₆₁BM weight ratio of 10/8, the film thickness of ca. 80 nm and solvent annealing in CHCl₃ saturated environment for 2 min. We then substituted PC₆₁BM with phenyl-C₇₁-butyric acid methyl ester (PC₇₁BM) in the **Pt-SM** devices by employing the optimized conditions. Table 1 summarizes the performance parameters of the devices and Figure 2 displays the representative I-V curves, and absorption and external quantum efficiency (EQE) profiles, as well as the transmission electron microscopy (TEM) image.

The optimized devices display an average PCE of ca. 5.6% and a highest value of ca. 5.9%, which are significantly higher than values reported previously for OSCs applying Pt-containing polymers. The J_{sc} values of **Pt-SM** devices are comparable to those reported previously for best-performing Pt-containing

polymers. The EQE responses closely match the thin film absorption profiles as shown in Figure 4A (insert), displaying panchromatic responses from 350 nm to 650 nm. A relatively large V_{oc} value of ca. 0.82 V was obtained, indicating small energy loss during the charge separation and collection processes, considering that the energy gap between HOMO of **Pt-SM** and LUMO of PC₇₁BM is ca. 1 eV.⁶⁴ These V_{oc} values are also comparable with those from the best performing devices employing Pt-containing polymers.

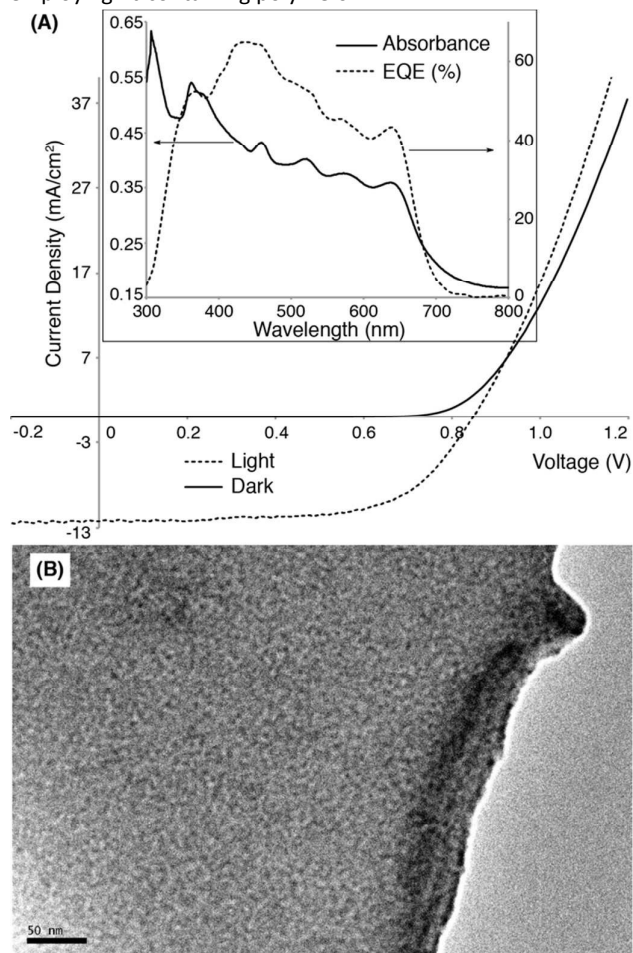


Figure 4. (A) Current density-voltage (I-V) curves of a representative OSC device in dark (solid line) and under simulated AM1.5 solar irradiation (dashed line). Inset: absorption (solid line) and external quantum efficiency (EQE, dashed line) profiles of the same device. (B) Transmission electron microscopy (TEM) image of the active layer of the device (scale bar is 50 nm).

The major improvement comes from the fill factors (*FFs*). **Pt-SM** devices constantly display *FFs* close to 60% while previous polymer examples rarely gave *FFs* above 40%. Furthermore, in previous examples, large excesses of fullerenes are required to reach the maximum *PCEs* due to the amorphous nature of the polymers. In the case of **Pt-SM**, only 44 wt.% of fullerenes are sufficient to achieve the optimum performance, likely due to the more crystalline nature of the small molecule leading to better thin film morphologies. Indeed, TEM image of the device active layer (Figure 4B) shows the absence of large aggregates and an interpenetrated network with favorable domain sizes of ca. 5–10 nm.

Table 1. Summary of OSC Device Performances Employing **Pt-SM** and PC₇₁BM.^[a]

Wt. Ratio ^[b]	J_{sc} (mA/cm ²) ^[c]	V_{oc} (V) ^[d]	FF (%) ^[e]	PCE (%) ^[f]	R_s (Ω cm ²) ^[g]	R_{sh} (Ω cm ²) ^[h]
10:8	11.9 ± 1.5 (14.4)	0.82 ± 0.03 (0.85)	57 ± 4.5 (63)	5.6 ± 0.29 (5.9)	5.6 ± 1.6	880 ± 520

[a] All devices employ **Pt-SM** and PC₇₁BM, adopting device structures: ITO glass/MoO₃ (10 nm)/organic blend layer (80 nm)/Al (100 nm), under simulated AM1.5 illumination. Average values and standard deviations are calculated from twelve individual devices, and the maximum values among tested devices are given in parentheses. [b] Weight ratio of **Pt-SM**/PC₇₁BM. [c] Short circuit current. [d] Open circuit voltage. [e] Fill factor. [f] Power conversion efficiency. [g] Series resistance. [h] Shunt resistance.

We then studied stability of the optimized **Pt-SM**/PC₇₁BM devices through aging tests at room temperature and at 80 °C, and the results are summarized in Figure S8 (see ESI[†]). After two weeks, the devices stored at room temperature show only slight decrease of performance to ca. 85% of the original PCEs; while devices kept at 80 °C display a bigger PCE drop to ca. 65%. From optical micrographs of these devices shown in Figure S9 (see ESI[†]), both devices as optimized and aged at room temperature show smooth films free of any visible phase segregation and large aggregates. Phase separations on the order of a few μ m can be observed in films aged at 80 °C after 14 days, which is still free of any large crystallites. Such coarsening of active layer morphologies likely explains the relatively higher decay rate of device performances.

Conclusions

In summary, we have designed and synthesized a Pt-bisacetylde containing SM, featuring "roller-wheel" geometry. This new structural design allows partial overlap among the main rigid chromophores, leading to enhanced crystallinity and π - π interactions. OSCs employing **Pt-SM** displayed higher PCEs, mostly resulted from improved FFs, than those applying Pt-containing polymers reported previously. This molecular design strategy can be extended to other low bandgap linear organic chromophores as well as conjugated polymers, which will potentially lead to promising materials for OSCs and other organic electronics.

Acknowledgements

The authors would like to acknowledge NSF (DMR-1453083) for financial support for this research. The Bruker X-ray diffractometer was purchased via an NSF CRIF:MU award to the University of New Mexico (CHE04-43580), and the NMR spectrometers were upgraded via grants from the NSF (CHE08-40523 and CHE09-46690). All DFT calculations were performed at the Center for Functional Nanomaterials, which is a U.S. DOE Office of Science Facility at Brookhaven National Laboratory under Contract No. DE-SC0012704.

Notes and references

1 F. C. Krebs; N. Espinosa; M. Hösel; R. R. Søndergaard; M. Jørgensen *Adv. Mater.* 2014, **26**, 29-39.

- 2 J. You; L. Dou; K. Yoshimura; T. Kato; K. Ohya; T. Moriarty; K. Emery; C.-C. Chen; J. Gao; G. Li; Y. Yang *Nat. Commun.* 2013, **4**, 1446.
- 3 B. Kan; M. Li; Q. Zhang; F. Liu; X. Wan; Y. Wang; W. Ni; G. Long; X. Yang; H. Feng; Y. Zuo; M. Zhang; F. Huang; Y. Cao; T. P. Russell; Y. Chen *J. Am. Chem. Soc.* 2015, **137**, 3886-3893.
- 4 Q. Zhang; B. Kan; F. Liu; G. Long; X. Wan; X. Chen; Y. Zuo; W. Ni; H. Zhang; M. Li; Z. Hu; F. Huang; Y. Cao; Z. Liang; M. Zhang; T. P. Russell; Y. Chen *Nat. Photon.* 2015, **9**, 35-41.
- 5 J. Zhang; Y. Zhang; J. Fang; K. Lu; Z. Wang; W. Ma; Z. Wei *J. Am. Chem. Soc.* 2015, **137**, 8176-8183.
- 6 X. Ouyang; R. Peng; L. Ai; X. Zhang; Z. Ge *Nat. Photon.* 2015, **9**, 520-524.
- 7 J. Subbiah; B. Purushothaman; M. Chen; T. Qin; M. Gao; D. Vak; F. H. Scholes; X. Chen; S. E. Watkins; G. J. Wilson; A. B. Holmes; W. W. H. Wong; D. J. Jones *Adv. Mater.* 2015, **27**, 702-705.
- 8 Y. Liu; Z. A. Page; T. P. Russell; T. Emrick *Angew. Chem. Int. Ed.* 2015, **54**, 11485-11489.
- 9 B. C. Thompson; J. M. J. Fréchet *Angew. Chem. Int. Ed.* 2008, **47**, 58-77.
- 10 Y. Huang; E. J. Kramer; A. J. Heeger; G. C. Bazan *Chem. Rev.* 2014, **114**, 7006-7043.
- 11 Y.-J. Cheng; S.-H. Yang; C.-S. Hsu *Chem. Rev.* 2009, **109**, 5868-5923.
- 12 H. Zhou; L. Yang; W. You *Macromolecules* 2012, **45**, 607-632.
- 13 L.-M. Chen; Z. Xu; Z. Hong; Y. Yang *J. Mater. Chem.* 2010, **20**, 2575-2598.
- 14 Z. A. Page; Y. Liu; V. V. Duzhko; T. P. Russell; T. Emrick *Science* 2014, **346**, 441-444.
- 15 T. Ameri; G. Dennler; C. Lungenschmied; C. J. Brabec *Energy Environ. Sci.* 2009, **2**, 347-363.
- 16 H. Zhou; Y. Zhang; C.-K. Mai; S. D. Collins; G. C. Bazan; T.-Q. Nguyen; A. J. Heeger *Adv. Mater.* 2015, **27**, 1767-1773.
- 17 C. J. Brabec; M. Heeney; I. McCulloch; J. Nelson *Chem. Soc. Rev.* 2011, **40**, 1185-1199.
- 18 A. J. Heeger *Adv. Mater.* 2014, **26**, 10-28.
- 19 A. Köhler; H. Bässler *J. Mater. Chem.* 2011, **21**, 4003-4011.
- 20 L. S. Devi; M. K. Al-Suti; C. Dosche; M. S. Khan; R. H. Friend; A. Köhler *Phys. Rev. B* 2008, **78**, 045210.
- 21 I. I. Fishchuk; A. Kadashchuk; L. S. Devi; P. Heremans; H. Bässler; A. Köhler *Phys. Rev. B* 2008, **78**, 045211.
- 22 S. T. Hoffmann; E. Scheler; J.-M. Koenen; M. Forster; U. Scherf; P. Strohriegel; H. Bässler; A. Köhler *Phys. Rev. B* 2010, **81**, 165208.
- 23 Y. Shao; Y. Yang *Adv. Mater.* 2005, **17**, 2841-2844.
- 24 H.-Y. Hsu; J. H. Vella; J. D. Myers; J. Xue; K. S. Schanze *J. Phys. Chem. C* 2014, **118**, 24282-24289.
- 25 Z. Chen; H.-Y. Hsu; M. Arca; K. S. Schanze *J. Phys. Chem. B* 2015, **119**, 7198-7209.
- 26 G. L. Schulz; S. Holdcroft *Chem. Mater.* 2008, **20**, 5351-5355.
- 27 M. Qian; R. Zhang; J. Hao; W. Zhang; Q. Zhang; J. Wang; Y. Tao; S. Chen; J. Fang; W. Huang *Adv. Mater.* 2015, **27**, 3546-3552.

- 28 K. Glusac; M. E. Köse; H. Jiang; K. S. Schanze *J. Phys. Chem. B* 2007, **111**, 929-940.
- 29 W.-Y. Wong *Macromol. Chem. Phys.* 2008, **209**, 14-24.
- 30 W.-Y. Wong; C.-L. Ho *Acc. Chem. Res.* 2010, **43**, 1246-1256.
- 31 W.-Y. Wong; X.-Z. Wang; Z. He; A. B. Djurisić; C.-T. Yip; K.-Y. Cheung; H. Wang; C. S. K. Mak; W.-K. Chan *Nat. Mater.* 2007, **6**, 521-527.
- 32 W.-Y. Wong; X.-Z. Wang; Z. He; K.-K. Chan; A. B. Djurisić; K.-Y. Cheung; C.-T. Yip; A. M.-C. Ng; Y. Y. Xi; C. S. K. Mak; W.-K. Chan *J. Am. Chem. Soc.* 2007, **129**, 14372-14380.
- 33 N. S. Baek; S. K. Hau; H.-L. Yip; O. Acton; K.-S. Chen; A. K.-Y. Jen *Chem. Mater.* 2008, **20**, 5734-5736.
- 34 L. Li; C.-L. Ho; W.-Y. Wong; K.-Y. Cheung; M.-K. Fung; W.-T. Lam; A. B. Djurisić; W.-K. Chan *Adv. Funct. Mater.* 2008, **18**, 2824-2833.
- 35 P.-T. Wu; T. Bull; F. S. Kim; C. K. Luscombe; S. A. Jenekhe *Macromolecules* 2009, **42**, 671-681.
- 36 F. Guo; Y.-G. Kim; J. R. Reynolds; K. S. Schanze *Chem. Commun.* 2006, 1887-1889.
- 37 J. Mei; K. Ogawa; Y.-G. Kim; N. C. Heston; D. J. Arenas; Z. Nasrollahi; T. D. McCarley; D. B. Tanner; J. R. Reynolds; K. S. Schanze *ACS Appl. Mater. Interfaces* 2009, **1**, 150-161.
- 38 W. He; Y. Jiang; Y. Qin *Polym. Chem.* 2014, **5**, 1298-1304.
- 39 K. Hu; E. Pandres; Y. Qin *J. Polym. Sci. A Polym. Chem.* 2014, **52**, 2662-2668.
- 40 B. Walker; C. Kim; T.-Q. Nguyen *Chem. Mater.* 2011, **23**, 470-482.
- 41 J. E. Coughlin; Z. B. Henson; G. C. Welch; G. C. Bazan *Acc. Chem. Res.* 2014, **47**, 257-270.
- 42 B. Kan; Q. Zhang; M. Li; X. Wan; W. Ni; G. Long; Y. Wang; X. Yang; H. Feng; Y. Chen *J. Am. Chem. Soc.* 2014, **136**, 15529-15532.
- 43 F. Guo; K. Ogawa; Y.-G. Kim; E. O. Danilov; F. N. Castellano; J. R. Reynolds; K. S. Schanze *Phys. Chem. Chem. Phys.* 2007, **9**, 2724-2734.
- 44 H. Zhan; S. Lamare; A. Ng; T. Kenny; H. Guernon; W.-K. Chan; A. B. Djurisić; P. D. Harvey; W.-Y. Wong *Macromolecules* 2011, **44**, 5155-5167.
- 45 J. E. Anthony; J. S. Brooks; D. L. Eaton; S. R. Parkin *J. Am. Chem. Soc.* 2001, **123**, 9482-9483.
- 46 J. E. Anthony *Chem. Rev.* 2006, **106**, 5028-5048.
- 47 M. Pope; C. E. Swenberg *Electronic Processes in Organic Crystals and Polymers*; Oxford University Press: New York, Oxford, 1999.
- 48 G. G. Dubinina; S. C. Price; K. A. Abboud; G. Wicks; P. Wnuk; Y. Stepanenko; M. Drobizhev; A. Rebane; K. S. Schanze *J. Am. Chem. Soc.* 2012, **134**, 19346-19349.
- 49 M. E. Casida In *Recent Advances in Density Functional Methods*; D. P. Chong, Ed.; World Scientific Publishing Co. Ltd.: Singapore, 1995, 155
- 50 R. Bauernschmitt; R. Ahlrichs *Chem. Phys. Lett.* 1996, **256**, 454-464.
- 51 M. J. Frisch; G. W. Trucks; H. B. Schlegel; et. al. GAUSSIAN 09, revision B.01, Gaussian, Inc., Wallingford, CT, 2010. <http://www.gaussian.com/>
- 52 P. J. Hay; W. R. Wadt *J. Chem. Phys.* 1985, **82**, 299-310.
- 53 J. Tomasi; B. Mennucci; R. Cammi *Chem. Rev.* 2005, **105**, 2999-3094.
- 54 R. L. Martin *J. Chem. Phys.* 2003, **118**, 4775-4777.
- 55 A cautionary note for this interpretation is that the calculated singlet excitation energies may be underestimated, especially considering the difficulty of TD-DFT with charge transfer states. See: A. Dreuw; M. Head-Gordon *J. Am. Chem. Soc.* 2004, **126**, 4007-4016.
- 56 S. C. Price; A. C. Stuart; L. Yang; H. Zhou; W. You *J. Am. Chem. Soc.* 2011, **133**, 4625-4631.
- 57 L. Huo; S. Zhang; X. Guo; F. Xu; Y. Li; J. Hou *Angew. Chem. Int. Ed.* 2011, **50**, 9697-9702.
- 58 H. J. Son; L. Lu; W. Chen; T. Xu; T. Zhang; B. Carsten; J. Strzalka; S. B. Darling; L. X. Chen; L. Yu *Adv. Mater.* 2013, **25**, 838-843.
- 59 L. Dou; W.-H. Chang; J. Gao; C.-C. Chen; J. You; Y. Yang *Adv. Mater.* 2013, **25**, 825-831.
- 60 F. C. Spano *Acc. Chem. Res.* 2010, **43**, 429-439.
- 61 F. C. Spano; C. Silva *Annu. Rev. Phys. Chem.* 2014, **65**, 477-500.
- 62 J. V. Caspar; B. P. Sullivan; E. M. Kober; T. J. Meyer *Chem. Phys. Lett.* 1982, **91**, 91-95.
- 63 P. N. Murgatroyd *J. Phys. D: Appl. Phys.* 1970, **3**, 151-156.
- 64 B. Qi; J. Wang *J. Mater. Chem.* 2012, **22**, 24315-24325.